heritage

MDPI

Article

Non-Invasive Analyses of Italian "Ostrogothic" Jewellery: The Desana Treasure

Maurizio Aceto [1,2,*], Elisa Calà [1,2], Francesca Robotti [1,2], Joan Pinar Gil [3], Simonetta Castronovo [4], Monica Gulmini [5], Maria Labate [5] and Angelo Agostino [5]

[1] Dipartimento per lo Sviluppo Sostenibile e la Transizione Ecologica, Università degli Studi del Piemonte Orientale, Piazza Sant'Eusebio 5, 13100 Vercelli, Italy
[2] Centro Interdisciplinare per lo Studio e la Conservazione dei Beni Culturali (CenISCo), Piazza Sant'Eusebio 5, 13100 Vercelli, Italy
[3] Katedra Archeologie, Univerzita Hradec Králové, Rokitanského 62, 50003 Hradec Králové, Czech Republic
[4] Museo Civico di Arte Antica, p.zza Castello, 10123 Torino, Italy
[5] Dipartimento di Chimica, Università degli Studi di Torino, Via P. Giuria 7, 10125 Torino, Italy
* Correspondence: maurizio.aceto@uniupo.it

Abstract: The Desana treasure is a remarkable assemblage of items made of gold, silver, gemstones and glasses found in north-western Italy. Most scholars agree on the fact that the core of the treasure might have belonged to a single deposit resulted from a long period of selection, accumulation and use. The treasure testifies to the evolution of goldsmiths' art in Ostrogothic Italy and represents an extraordinary material trace of the Italian elites of the 5th–6th centuries. The Desana treasure was investigated with non-invasive instrumental analytical techniques, namely optical microscopy, UV-visible diffuse reflectance spectrophotometry with optical fibres and X-ray fluorescence spectrometry in order to record the chemical features of gemstones, coloured glasses and precious metals employed to produce the items. As for the gemstones, besides identifying typologies, data suggested India as the source for a sapphire pendant and for most of the garnets, whereas the emeralds may belong to different sources, among which Pakistan, India and Egypt. The investigation revealed the colouring agents and compositional features of the glasses, and the composition of the gold alloys. The results of the investigation highlight that the raw materials used by Late Antique Italian goldsmiths did not differ significantly from other neighbouring European and Mediterranean regions, although the garnets show some differences if compared with coeval jewels recorded north of the Alps. The dataset produced in this work complements the stylistic approach for the study of these amazing traces of the past and deepens our knowledge on the role of the Italian "Ostrogothic" jewellery in the frame of the coeval Mediterranean, Central European and Northern Pontic metalwork traditions.

Keywords: jewellery; XRF; FORS; Ostrogothic jewellery; Desana; Piemonte

Citation: Aceto, M.; Calà, E.; Robotti, F.; Gil, J.P.; Castronovo, S.; Gulmini, M.; Labate, M.; Agostino, A. Non-Invasive Analyses of Italian "Ostrogothic" Jewellery: The Desana Treasure. *Heritage* **2023**, *6*, 1680–1697. https://doi.org/10.3390/heritage6020089

Academic Editor: Craig J. Kennedy

Received: 31 December 2022
Revised: 24 January 2023
Accepted: 1 February 2023
Published: 4 February 2023

1. Introduction

The so called "Ostrogothic" precious metal deposits show a prominent position among the material traces of the Italian elites of the 5th and 6th centuries. As such, they encompass fundamental information on the material culture, the visual appearance and the networking strategies of these social groups that has drawn the attention of different generations of archaeologists and art historians [1–7].

One of the most prominent representatives of these deposits is the so called Desana treasure, a remarkable assemblage of objects made of gold, silver and gemstones found in an undetermined spot between the towns of Desana and Trino Vercellese (nowadays Vercelli province, Piemonte region, north-western Italy) [7]. Acquired through antiquities trade in 1938 by the City Museum of Ancient Art in Turin, it is not possible to determine to what extent the assemblage retains its original integrity. There is, however, a wide scholarly consensus on the fact that the core of the treasure might have belonged to a

single deposit, as some witnesses of the discovery attest. Of paramount importance in this background is the recording of similar assemblages of objects in well-recorded stratigraphical contexts of northern Italy. Among them, the Reggio Emilia treasure, concealed in a reused lead pipe under the floor of a late Roman house, deserves a particular mention, as the typological repertory of the objects and the chronology are particularly close to the Desana treasure [1,8].

The comparison of the Reggio Emilia and Desana treasures, along with other similar collections, indicates that they might have resulted from prolonged and intricate processes of object accumulation, selection, and utilisation, with a main focus during 470-530 CE [7,8]. Objects rooted in Mediterranean, Central European and Northern Pontic metalwork traditions can be identified in both deposits, although in most of the cases their precise place of manufacture is still unknown. At Desana, for instance, the pair of *cloisonné* bow brooches (30/Ori and 31/Ori), the two silver crossbow brooches (380/A and 381/A), the composite belt buckle with cabochons (382/A) and the necklace with cabochons (20/Ori) can be safely attributed to Italian production centres based on the geographical distribution of their closest parallels. Other objects, instead, cannot be connected yet to a specific place or region within the Mediterranean basin.

The Desana treasure, thus, shows several exceptional features:

1. it derives from a long and complex period of selection, accumulation and use;
2. it provides a consistent sample of the main regional guidelines in the evolution of jewellery over more than one hundred years;
3. it displays evident connections with «global» fashions, to their production centres and to the trade networks lying underneath them.

The latter point is a crucial one on a European-wide level. The jewellery of the 5th–6th centuries show an unprecedented use of gemstones originating from distant, often extra-European outcrops. An example is the group of jewellery of the Apahida–Tournai group, probably manufactured in Constantinopolitan workshops, in which garnets of Asian and Bohemian origin were common raw materials [9]. The stylistic affinities between the Italian "Ostrogothic" jewellery, on the one hand, and the goldsmithing masterpieces of the Apahida–Tournai group, on the other, are widely acknowledged by archaeologists and art historians alike. However, how the Italian jewellery of that time interacted with the productions of coeval "fashion metropolises" remains unclear due to the lack of large-scale systematic analyses of the composition of the artefacts found south of the Alps.

In such a background, the preliminary inspection by optical microscopy, UV-visible diffuse reflectance spectrophotometry with optic fibres (FORS) and the determination of the elemental composition by X-ray Fluorescence spectrometry (XRF) of the Desana treasure presented in this paper put together a relevant dataset to characterise the technology and raw materials used in the jewellery of the 5th–6th centuries found in present-day Italy.

A collection of artefacts from archaeological deposits recorded throughout northern Italy is currently under study with non-invasive diagnostic techniques, in order to characterise the materials with which the items were produced and to gain information on the source of raw materials.

2. Materials and Methods

2.1. UV-Visible Diffuse Reflectance Spectrophotometry with Optic Fibres (FORS)

FORS analysis was performed with an Avantes (Apeldoorn, The Netherlands) AvaSpec-ULS2048XL-USB2 model spectrophotometer and an AvaLight-HAL-S-IND tungsten halogen light source; detector and light source were connected with fibre optic cables to an FCR-7UV200-2-1,5x100 probe. In this configuration, both the incident and detecting angles were 45° from the surface normal in order not to include specular reflectance. The investigated area on the sample had a 1 mm diameter. The probe was held by hand in contact with the sample, and the tip of the probe was covered with a small cylindrical sheath properly cut to fit the measurement angle in order to exclude external light. The spectral range of the detector was 200–1160 nm; the overall operational range of the device

(combination of lamp + detector) was 375–1100 nm. Depending on the features of the monochromator (slit width 50 μm, grating of UA type with 300 lines/mm) and of the detector (2048 pixels), the best spectra resolution was 2.4 nm calculated as FWHM. Diffuse reflectance spectra of the samples were referenced against the WS-2 reference tile provided by Avantes and guaranteed to be reflective at 98% or more in the investigated spectral range. The instrumental parameters were as follows: 10 ms integration time and 100 scans for a total acquisition time of 1.0 s for each spectrum. The whole system was managed by the AvaSoft v. 8 dedicated software, running under Windows 7.

2.2. X-ray Fluorescence Spectrometry (XRF)

XRF measurements were performed with an EDXRF Thermo (Waltham, MA, USA) NITON spectrometer XL3T-900 GOLDD model, equipped with an Ag tube (max. 50 kV, 100 μA, 2 W), a large area Silicon Drift Detector (SDD), with an energy resolution of about 136 eV at 5.9 keV. The analysed spot had an average diameter of 3 mm and was focused by a CCD camera with a working distance of 2 mm. Total time of analysis was 240 s with two different conditions and algorithms: "Metal" for the alloys and "Mining" for glasses and gemstones. The instrument was held in position with a moving stage allowing micrometric shifts in order to reach the desired probe-to-sample distance; the stage was laid on a tripod. The obtained spectra were processed with the commercial software BAxil (Brightspec NV/SA, Belgium) derived from the academic software QXAS from IAEA. As a distinction exists between heavy matrices (metal alloys) and light matrices (glass and gemstones), two different quantification models were applied, both based on the fundamental parameter model of De Jongh improved by the use of appropriate certified reference materials (ARMI MBH, Manchester, NH, USA; The XRF Company, Houston, TX, USA; NIST, Gaithersburg, MD, USA; SGT, Sheffield, UK; Corning, NY, USA). The precision of the measurements can be estimated between 3% for transition and heavy metals and 5% for light elements. The accuracy and precision of the measurements was found to be adequate to distinguish compositional groups of glass materials, as shown in the recent work of Yatsuk et al. [10] and of materials with siliceous base such as most of the gemstones identified in this work. The detection limits, calculated on the ability to obtain an integrated area value 3σ higher than the background noise around the signal relative to individual elements, may be summarised as follows for measurable elements (atomic weight > Mg):

- ~30 ppm for elements >Fe;
- 100 ppm for elements between Cl and Mn;
- 150 ppm for S (in absence of Pb);
- 300 ppm for P;
- 3000 ppm for Si;
- 6000 ppm for Al;
- 5% for Mg (excluded from processing in this work).

2.3. Optical Microscopy

A USB Dino-Lite (New Taipei City, Taiwan) AM4113T-FV2W model microscope was used to acquire digital images at 50× and 200× magnification. The instrument is equipped with 375 nm and visible LED lights and a digital camera with 1.3 Megapixel resolution.

3. Results

The measurements were carried out on three types of materials:

- the gemstones, present in blue, green, red and violet colours;
- the glasses, present in blue and green colour;
- the gold alloys.

The gemstones and the glasses were analysed by means of FORS and XRF. The gold alloys were analysed by means of XRF only.

3.1. Gemstones

The identification of the gemstones was performed through the features of the FORS spectra [11]. It must be noted that the relevant features in the reflectance mode are the minima in the spectrum, which are related to the absorption properties of the material in the investigated spectral range. Reflectance maxima are instead related only to the perceivable colour of the gemstones. Therefore, in the following sections the spectra are reported in Log(1/reflectance) coordinates, also called *apparent absorbance*, in order to highlight the absorption features as maxima in the spectra. Moreover, an offset was applied along the Y axis in order tto facilitate comparison between the spectra. According to the absorption features, it was possible to identify all the typologies of the gemstones present in the investigated items.

XRF analyses contributed further hints for placing the origin of the gemstones from a geochemical perspective. Accuracy and precision of XRF data with portable equipment were recently investigated throughout for archaeological glass [10] and can be considered here to evaluate the quality of the elemental determinations. A precision of 3–5% was determined for the concentrations in the gemstones.

3.1.1. Blue Gemstones

Only one true blue gemstone, a drop stone in a pendant earring (object no. 16/Ori), was present. This was identified as a sapphire. The identification relied on the absorption band at 453 nm due to Fe^{3+} ions, on the broad absorption band centred at 560 nm and assigned to Fe^{2+}/Ti^{4+} intervalence charge transfer, and on the two luminescence bands at 693 and 694 nm, due to Cr^{3+} ions, here appearing as a single sharp negative band in the FORS spectrum (see Figure 4 in Section 3.2.1) [11]. Under the optical microscope, the sapphire appears to be ground and then drilled; considering the hardness of the stone (9/10 on the Mohs scale), this work must have been done with diamonds (10/10 on the Mohs scale), employing a technology that, in antiquity, was documented only in India [12,13]. This feature suggests a recycle of Roman material [14]. In addition, the lack of the absorption band at 880 nm, assigned to Fe^{2+}, is usually taken as a clue for the metamorphic origin of the gemstone, rather than basalt-related [15,16], which would include Madagascar, Sri Lanka and Vietnam as possible geographic sources. Considering that the only active deposits in the Middle Ages were in Myanmar, Sri Lanka, and Thailand-Cambodia [17], an origin from south-eastern Asia is highly probable. The Greek writer, traveller and merchant Cosmas Indicopleustes, in his 6th century *Christian Topography* [18] cited the island of Taprobane, modern Sri Lanka, as the source of "hyacinth stone", interpreted as sapphire or as amethyst. Another important historical source confirming the same geographic origin is the 11th century treatise on gems by Abu al-Rayhan Mohamed ibn Ahmad al-Biruni, a philosopher, traveller and scientist with direct knowledge of the Indian and Sinhalese deposits [19,20].

As far as the elemental composition is concerned, XRF analysis showed only the presence of impurities of Fe (0.06%), Ti (0.03%) and Ga (0.01%). The concentration of trace elements sometimes can be used to trace the geographic provenance of corundum gemstones, as discussed by Barone et al. [20]. As an example, Kochelek et al. [21] identified the sources of rubies and sapphires by means of their elemental composition determined by Laser-induced breakdown spectroscopy (LIBS) coupled with multivariate analysis of data. Unfortunately, this approach, which is micro-invasive and micro-destructive, was not allowed in the present study, and only non-invasive analyses were permitted.

3.1.2. Green Gemstones

The green gemstones were the most abundant. They were present in the following items:

- a rod bracelet (object no. 8/Ori);
- a bracelet with articulated elements (object no. 10/Ori);
- a pendant earring (object no. 16/Ori);
- a ring with a smooth emerald (object no. 19/Ori);

- a necklace (object no. 20/Ori);
- a fragment of necklace (object no. 21/Ori);
- a ring with a carved emerald (object no. 29/Ori).

The total number of green gemstones in the considered items was 52, 43 of which were placed on object no. 8/Ori. All of them showed the typical spectral features of emerald [11] with absorption bands at 420–440, 607–625 and 830–862, and shoulders at 640 and 680 nm (Figure 1). Despite a certain variability in the positions of the three main bands, it was not possible to identify specific groups. The strong absorption at 830–862, due to Fe^{2+} ion, according to the scientific literature [22–24], allows for exclusion of a modern source such as Colombia for these emeralds, which would have involved a posthumous replacement of the gemstones.

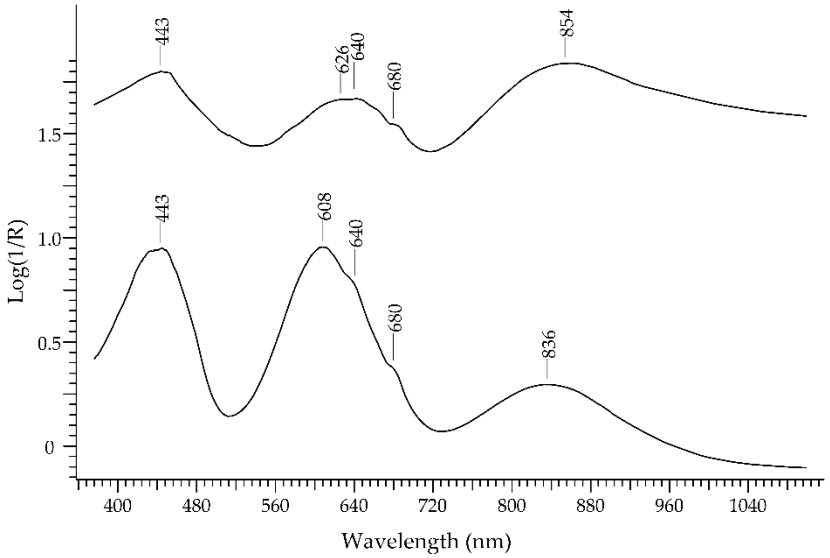

Figure 1. FORS spectra in Log(1/R) coordinates of two emeralds.

XRF confirmed that the Fe content was significant, ranging from 0.48 to 1.22% as FeO. In addition, the Cr/V ratio ranged from 2.8 to 12.3, whereas Colombian emeralds are characterised by a Cr/V ratio <1, as suggested by Karampelas et al. [24]. The role of trace element distribution in determining the geographic source of emeralds has been recently discussed [24–26]. Making reference also to older studies [27,28], it is possible to formulate some hypotheses on the sources of the emeralds of the Desana treasure. The elemental composition is variable, so it seems the gemstones could come from different sources:

- the emeralds of the bracelets no. 8/Ori and no. 10/Ori appear to have a composition matching the Pakistani quarries, according to the content of Fe (respectively 1.11 and 1.22% as FeO) and Cr (0.84 and 0.95% as Cr_2O_3);
- the emeralds of the earring no. 16/Ori, the ring no. 19/Ori and the necklace no. 20/Ori have a composition fitting the Egyptian origin;
- the emerald of the ring no. 29/Ori has a composition resembling that of an Indian source;
- finally, the three emeralds of the necklace no. 21/Ori show three apparently different compositions, compatible, respectively, with Egyptian, Indian and Austrian (Habachtal) sources.

Apart from the Austrian one, all other sources appear to be compatible with the information reported in ancient treatises. Pliny the Elder, in Book 37, lines 65–76 of the *Natural Historia* [29] explicitly cites Egypt, Ethiopia, Bactria (Pakistan and Afghanistan), India and Scythia (probably the Urals) as the sources of the emeralds exploited by Romans.

3.1.3. Red Gemstones

The red gemstones were almost ubiquitous in the Desana treasure. They were present in the following items:

- a rod bracelet (object no. 8/Ori);
- a bracelet or diadem with articulated elements (object no. 10/Ori);
- a pair of polyhedral earrings (object no. 13/Ori);
- a necklace (object no. 20/Ori);
- a ring with engraved garnet (object no. 23/Ori);
- a ring with smooth garnet (object no. 24/Ori);
- a *cloisonné* bow brooch (object no. 30/Ori);
- a *cloisonné* bow brooch (object no. 31/Ori);
- a gold bezel with garnet (object no. 135/Ori);
- a belt buckle (object no. 382/A).

The total number of red gemstones was 37, 22 of which were placed on object no. 8/Ori. In addition, many red *cloisonné* pieces were found in the two bow brooches, objects no. 30/Ori and 31/Ori. All these gemstones showed the typical spectral features of garnet [11] with absorption bands at 407/505/521/567/611/691 nm, which are typical of the pyrope-almandine variety (Figure 2). A few garnets showed an additional band at 454 nm. The high number of garnets is coherent with the fact that this was the dominant gem mineral in jewellery in the Early Middle Ages [30].

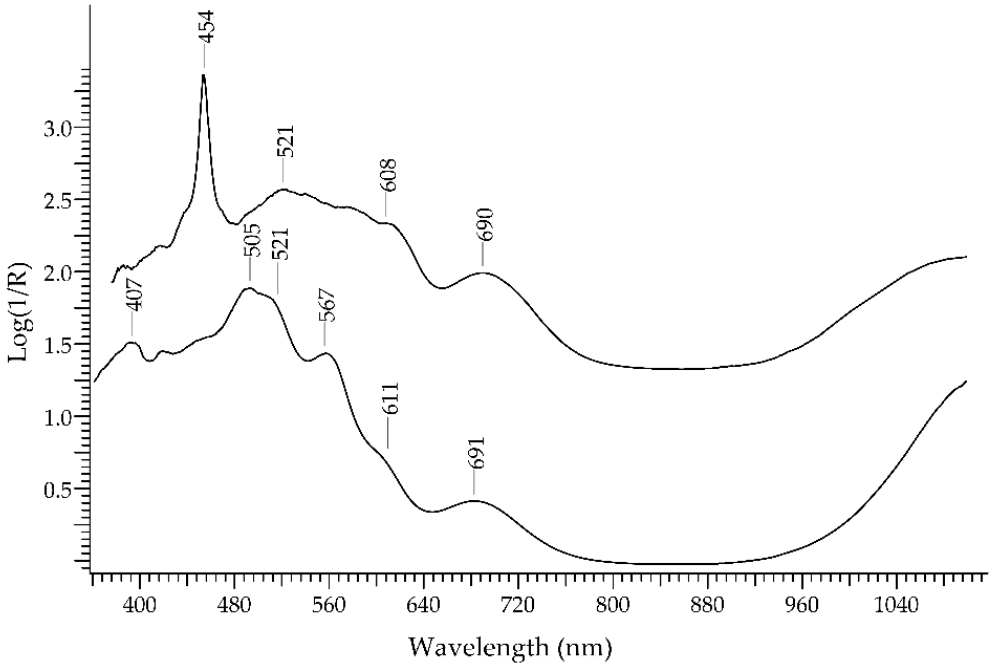

Figure 2. FORS spectra in Log(1/R) coordinates of two garnets.

Apart from the identification of the red gemstones as garnets by FORS, XRF analysis can add some information on their geographic provenance, as the elemental composition, from major to trace elements, can give some suggestions on the possible source of the gemstones. The data obtained here for the Desana treasure can in fact be interpreted in the light of those already available in the scientific literature and particularly with the data resumed in the recent exhaustive work by Pion et al. [31]. The authors analysed thousands of garnets by means of Proton Induced X-Emission (PIXE) spectroscopy and were able to classify them into six groups, according to the elemental distribution:

- type I, almandine from Rajasthan, India;
- type II, calcium-rich almandine from India;

- type IIIA, calcium-poor pyrope-almandine from Central Sri Lanka;
- type IIIB, calcium-poor pyrope-almandine from South Sri Lanka;
- type IV, chrome poor pyrope from Monte Suímo, Portugal;
- type V, chrome-rich pyrope from Bohemia, Czech Republic.

Despite the difference in the technique used for gaining elemental data (XRF vs. PIXE), a comparison can nevertheless be made. The elemental composition of the garnets contained in the objects no. 8/Ori, no. 13/Ori, 23/Ori, 24/Ori and 30/Ori is close to types I and II, as can be seen in Table 1; the most important elements in this classification are Fe, which is higher in types I and II than in the other groups, and Cr and Mg which on the contrary are lower. It must be noted that the LOD (limit of detection) [32,33] for Mg of the portable XRF instrument used in this work is 8% expressed as MgO; therefore, we can safely exclude that these garnets belong to type IV and V, as an MgO content higher than 10% was excluded.

Table 1. Elemental content of the garnets expressed as% oxide.

Element	8/Ori, 13/Ori, 23/Ori, 24/Ori and 30/Ori	10/Ori	20/Ori	Type I [1]	Type II [1]	Type IV [1]	Type V [1]
SiO_2	32.8–42.8	61.13	47.73	36.0	37.3	41.2	41.5
FeO	27.8–41.7	12.61	16.83	37.5	32.1	12.7	8.9
Al_2O_3	16.2–19.9	13.03	25.37	20.8	21.5	23.1	21.6
MgO	<LOD	<LOD	<LOD	4.4	6.2	16.3	19.8
CaO	0.6–5.9	3.04	6.71	0.7	1.4	5.4	4.3
MnO	0.3–2.1	0.45	0.40	0.4	1.2	0.4	0.3
Cr_2O_3	0–0.2	<LOD	0.04	0.0	0.1	0.0	2.2
TiO_2	0–1.2	<LOD	0.60	0.0	0.0	0.4	0.5
CuO	0–0.4	1.39	<LOD	[2]	[2]	[2]	[2]
NiO	0–0.04	1.95	0.02	[2]	[2]	[2]	[2]
Y	0–0.06	<LOD	0.013	[2]	[2]	[2]	[2]

[1] Data from Pion et al. [31] (p. 842). [2] Data not available in the literature.

Quite similar results were found by Gilg et al. [34] on an Early Byzantine almandine garnet dated to 6th–8th century and assigned by the authors to the Coromandel Coast in south-eastern India. These data led us to hypothesise that these garnets came from the Indian subcontinent. This is not a surprising result, indeed. Again making reference to the descriptions of Cosmas Indicopleustes, he reported on the export of "alabandenum" (interpreted as almandine garnet) to the Mediterranean region from a port named "Caber", historically associated with the harbour of Kaveripattinam on the Coromandel coast and cited also by Ptolemy as the "Kaberis Emporium" [35]. According to the work of Pion et al. [31] (pp. 846–847), almandine garnets coming from south-eastern Asia (mostly of types I and II) accounted for the majority of uses until the late 6th century AD, to be replaced later on by type IV and type V European pyrope garnets. For example, the composition of the garnets present in the Visigothic *treasure of Guarrazar* (Spain, 7th century) has been found to be compatible with a type IV (Monte Suímo, Portugal) origin [27].

The garnet contained in the object no. 20/Ori is instead close to type IV according to a higher content of Al_2O_3 and CaO and a lower content of FeO. Finally, for the garnet contained in the object no. 10/Ori a proper comparison cannot be found, due to an unusually high content of SiO_2. To the best of our knowledge, similar compositions have not been recorded in any other jewel surely dating from the 5th–6th centuries. Provided that 10/Ori was an old object at the time of the treasure's concealment and that 20/Ori embodies recycled old gemstones, the XRF data suggest that these garnets may have a different chronology than the objects containing Indian garnets.

Due to the unfavourable arrangement of the gemstones in the metalwork, it was not possible to analyse with XRF the garnets in the objects no. 135/Ori and no. 382/A. The *cloisonné* garnets contained in the bow brooch no. 31/Ori showed the same features of those contained in the bow brooch no. 30/Ori.

3.1.4. Violet Gemstones

The violet gemstones are present in three items:

- a bracelet with articulated elements (object no. 10/Ori);
- a bulla-shaped *capsella* (object no. 11/Ori);
- a necklace (object no. 20/Ori).

A total of 16 gemstones are present, 3 on object no. 10/Ori, 11 on object no. 11/Ori and 2 on object no. 20/Ori. All these gemstones yielded the same spectrum (Figure 3) characterised by a single wide absorption band between 535 and 550 nm and a weak band between 900 and 950 nm. This is the typical feature of amethyst [11], due to Fe^{3+} impurities exposed to ionising radiation.

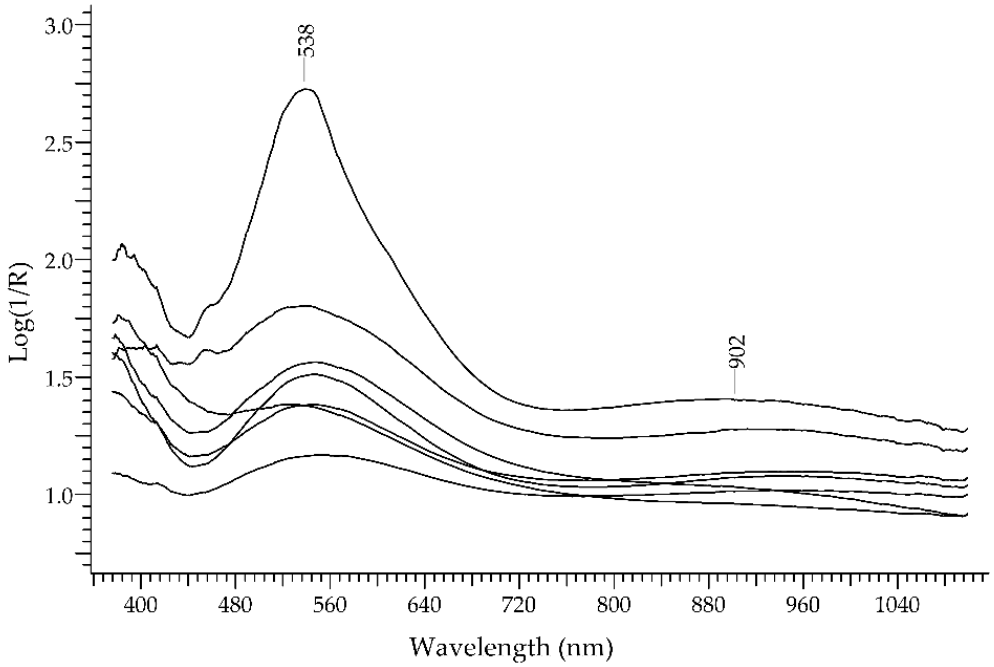

Figure 3. FORS spectra in Log(1/R) coordinates of some amethysts.

Elemental analysis by means of XRF did not highlight any geochemical fingerprint. Impurities of Al, Ca, Fe and Cu were found to be lower than 0.5% (as element oxides).

3.1.5. Other Gemstones

The bracelet with articulated elements (object no. 10/Ori) contained a further gemstone with a very dark blue colour, hardly perceivable on sight. The resulting FORS spectrum, however, did not evidence clearly the typical features of sapphire. The absorption band at 560 nm related to Fe^{2+}/Ti^{4+} intervalence charge transfer was negligible, and neither the bands at 453 nm (Fe^{3+}) and 880 nm (Fe^{2+}), nor the luminescence bands at 693/694 (Cr^{3+}), were present. XRF analysis showed a composition partially compatible with a corundum: Al_2O_3 92.7%, SiO_2 5.77%, with FeO (0.53%) and ZrO_2 (0.79%) as minor components. The gemstone could therefore be identified tentatively as a sapphire, but further investigation will be needed to fully understand its chemical nature. Krzemnicki et al. [36] reported on a Roman sapphire intaglio with fairly similar spectral features. The authors attributed this behaviour to Rayleigh scattering by sub-microscopic particles within the sapphire, rather than to absorption properties. As scattering effects are well known both in metamorphic and in basaltic sapphires [37,38], it would not be possible to draw a hypothesis on the origin of this particular gemstone.

An uncoloured gemstone was present on the ring no. 22/Ori. The data arising from XRF analysis allowed to identify it as a quartz.

3.2. Glasses

The presence of glassy gemstones in place of true gemstones may seem to decrease the overall value of the items, but glasses and vitreous pastes were indeed commonly used in medieval jewellery, as attested in several works [9,39–42]. Moreover, it is probable that during Late Antiquity and the Middle Ages, glass was considered a material of higher value than today. In some cases, it is possible to hypothesise that these glasses were a replacement of lost gemstones.

Blue and green glasses are present in the different objects of the treasure.

3.2.1. Blue Glasses

Four blue glasses resulted to be present in the following items:

- the eye of the griffin in the cochlear (object no. 379/A);
- the eye of the fish in a *ligula* (object no. 364/A);
- two eyes on tip in a *ligula* (object no. 364/A).

All these pieces yielded the same FORS spectra, shown in Figure 4, characterised by a wide absorption band structured into three sub-bands with maxima at 533, 595 and 642 nm: this is the typical spectral fingerprint of a blue glass coloured with Co^{2+} ions.

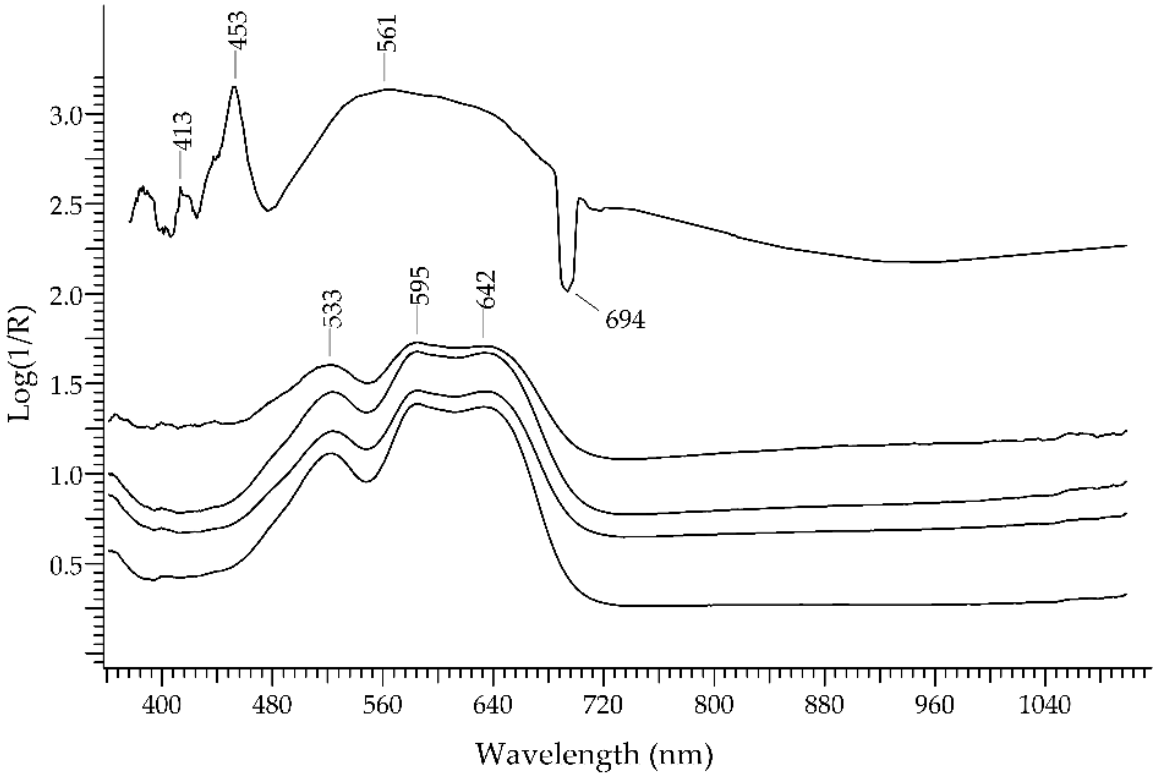

Figure 4. FORS spectra in Log(1/R) coordinates of the blue gemstone (top spectrum) and the blue glasses (bottom spectra).

Unfortunately, the very small size of the blue glasses and their position inside the metal objects prevented the possibility to record accurate data for XRF analysis.

3.2.2. Green Glasses

FORS spectra and XRF analyses confirmed that, as previously proposed [7], all the dark green *cloisonné* pieces on the two bow brooches (objects no. 30/Ori and 31/Ori) were green glasses.

Similarly, green glasses were present in the following items:

- a rod bracelet (object no. 8/Ori);

- the eye of the fish in a *ligula* (object no. 362/A);
- the eye of the fish in a *ligula* (object no. 363/A).

All the green glasses showed a wide absorption band with a maximum ranging from 715 nm to 800 nm (Figure 5), suggesting the presence of Cu^{2+} as the chromophore ion. One *cloisonné* piece on the bow brooch 31/Ori had an unusual turquoise hue and showed a much higher reflectance, suggesting that it was possibly later replacement.

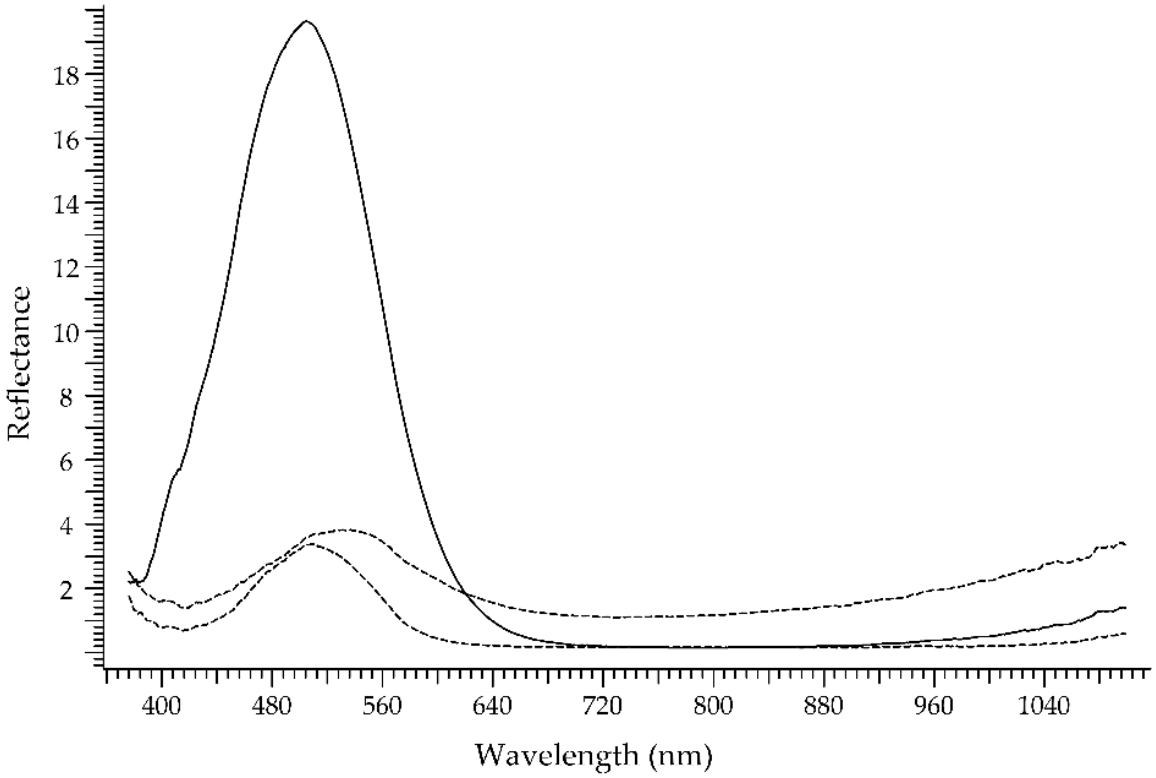

Figure 5. FORS spectra in reflectance coordinates of two green glasses (dashed line) and a possible replacement (solid line) of the bow brooch 31/Ori.

Two green glasses were present on the rod bracelet (object no. 8/Ori) possibly as replacements of lost emeralds. XRF analysis showed that these stones were indeed vitreous pastes, according to the content of SnO_2 (2.5%) and Sb_2O_5 (0.6%). The colourant was Cu^{2+} (1.5% as CuO), as already suggested by FORS analysis. The content of PbO was very high (29.0%). The composition is reported in Table 2.

Table 2. Elemental content of the green vitreous pastes on object no. 8/Ori, expressed as% oxide.

Element	8/Ori
SiO_2	49.0
PbO	29.0
CaO	3.4
SnO_2	2.5
K_2O	2.4
Cl	1.9
CuO	1.5
FeO	0.90
Al_2O_3	0.3
Sb_2O_5	0–0.04

The high value of the K_2O/CaO ratio, combined with the high PbO content, suggest that this glass has been introduced as a replacement at least in the 19th century. This would imply that the missing emeralds were replaced after the modern discovery of the deposit.

The dark green *cloisonné* pieces on the two bow brooches no. 30/Ori and 31/Ori showed a high content of SiO_2 (68.6% on average). They were typical soda-lime glasses, with 7.3% CaO and K_2O lower than 1% (the content of Na_2O cannot be determined with the instrument used in this work). The content of CuO was 2.3% on average. FeO, MnO and Al_2O_3 were, respectively, 3.2%, 1.3% and 2.6%.

The eyes of the fish in the ligulas no. 362/A and 363/A were too small to be analysed by means of XRF.

3.3. Gold Alloys

XRF spectrometry, a technique that has now reached an excellent level of accuracy, can supply the quantitative compositions of precious alloys and at the same time be used directly in situ in a non-invasive way.

The portable instrumentation has been successfully used in other analytical campaigns and the versatility of the non-invasive XRF approach has enabled chemical information to be obtained without the invasivity of a traditional metallographic approach. Obviously, the collected data are representative of the average value for the composition of the alloy and can be influenced by the condition of the surface layer. In fact, as reported in many studies concerning the chemical analysis of precious alloys [43,44], it is known that a selective loss of some elements generates a surface enrichment of the others, resulting in an erroneous evaluation of the original composition.

In addition to the artefacts mentioned above, the Au alloys of the following objects were analysed:

- an openwork bracelet (object no. 9/Ori);
- a crossbow brooch (object no. 12/Ori);
- a pair of polyhedral earrings (object no. 14/Ori);
- a pair of wire earrings (object no. 17/Ori);
- a fragmentary wire earring (object no. 18/Ori);
- a wedding ring (object no. 25/Ori);
- a cross-shaped pendant (object no. 26/Ori);
- a finger ring with personal name (object no. 27/Ori);
- a finger ring with monogram (object no. 28/Ori).

The phenomenon of copper depletion in precious alloys Ag/Cu or Au/Ag/Cu is always present, especially if the contents of this metal are very high [44,45]. As a consequence, the migration of copper from the alloy to the external environment affects the quantitative result of the XRF analysis resulting in an erroneous overestimation of precious metals (gold or silver) in the surface alloy. Fortunately, in the items of the present study, this phenomenon is almost negligible because the state of conservation of the objects and their production period leads to exclude high levels of copper and possible phenomena of decreasing.

The analysis of the gold alloys showed a substantial consistency with the typical compositions of the period (Table 3). The percentages of Au, Ag and Cu (marked box) were the normalised values of the precious alloys, while the percentages of Fe, Pb, Zn were the values of external components.

These were almost exclusively gold, silver and copper ternary alloys with accessory phases often below the detection capabilities of XRF and certainly below the LOD, which for these elements was commonly around 100 ppm.

The presence of iron is mainly attributable to anthropogenic contamination, due for example to the processing (such as brushing) and finishing phases [46].

The object 12/Ori must be considered a case apart, as the presence of iron, copper and zinc was to be attributed to the complex structure of the clasp. It is a composite object in which iron inserts are incorporated in the gold body. The melting medium used for

welding parts is lead. In fact, if disassembled it looks like the union of a pin screwed to the body of the clasp. The pin looks like a screw with a head made of gold alloy (Au/89%, Ag/9%, Cu/2%) to the base of which is anchored an iron core surmounted by a thread with the same composition of the head. The threaded cavity that holds the screw is again formed by the assembly of a hollow cylinder in gold with a small iron ring inside.

All the objects showed limited compositional variations, which allowed us to identify some groups of similarities. Data were subjected to Principal Components Analysis (PCA), in order to highlight groups of items with similar composition (Figure 6).

Table 3. Elemental composition of the alloy in wt/wt%.

Item Analysed	Au	Ag	Cu	Fe	Pb	Zn
8/Ori	92.3	5.2	1.6	1.3	0.0	0.0
9/Ori	91.7	7.2	1.1	0.2	0.0	0.0
10/Ori	92.2	7.1	0.7	0.1	0.0	0.0
11/Ori	91.2	7.7	1.1	0.1	0.0	0.0
12/Ori	91.4	7.4	1.3	0.2	0.0	0.0
12/Ori screw	88.8	8.7	2.5	11.5	0.6	0.0
12/Ori screw core	86.1	4.6	9.3	2.8	19.2	1.6
12/Ori screw inside c	88.4	8.6	3.0	9.1	0.3	0.0
12/Ori screw head	88.9	9.2	1.9	0.3	0.0	0.0
13/Ori	94.5	4.1	1.4	0.1	0.0	0.0
14a/Ori	93.6	3.3	3.1	0.7	0.5	0.0
14b/Ori	93.0	3.4	3.6	0.2	0.0	0.0
15a/Ori	85.0	10.3	4.7	0.6	0.0	0.0
15b/Ori	87.1	10.8	2.1	0.0	0.0	0.0
16/Ori ring	86.4	12.0	1.5	0.1	0.0	0.0
16b/Ori pendant	89.6	6.5	4.0	0.5	0.0	0.0
16b/Ori pendant	91.4	5.8	2.9	0.2	0.0	0.0
16b/Ori pendant	91.3	6.5	2.2	0.2	0.0	0.0
17a/Ori	92.2	5.8	2.0	0.3	0.0	0.0
17b/Ori	92.2	5.7	2.0	0.2	0.0	0.0
18/Ori	75.5	22.6	1.8	0.0	0.0	0.0
19/Ori	84.4	12.0	3.6	0.8	0.0	0.0
20/Ori	81.4	15.6	3.0	0.1	0.0	0.0
21/Ori	84.4	12.0	3.6	0.5	0.0	0.0
22/Ori	83.8	13.0	3.3	0.2	0.0	0.0
23/Ori	86.7	5.4	7.9	0.3	0.0	0.0
24/Ori	83.5	12.3	4.2	0.1	0.0	0.0
25/Ori	86.0	12.4	1.6	0.1	0.0	0.0
25/Ori cartouche edge	88.5	9.9	1.6	1.1	0.0	0.0
25/Ori inscription	84.7	12.1	3.3	1.9	0.0	0.0
26/Ori	83.5	11.5	5.0	0.3	0.0	0.0
27/Ori	90.2	9.1	0.7	0.5	0.0	0.0
28/Ori	87.3	9.8	2.9	1.1	0.0	0.0
29/Ori	95.6	3.7	0.7	0.1	0.0	0.0
30/Ori	82.8	11.8	5.3	0.6	0.0	0.0

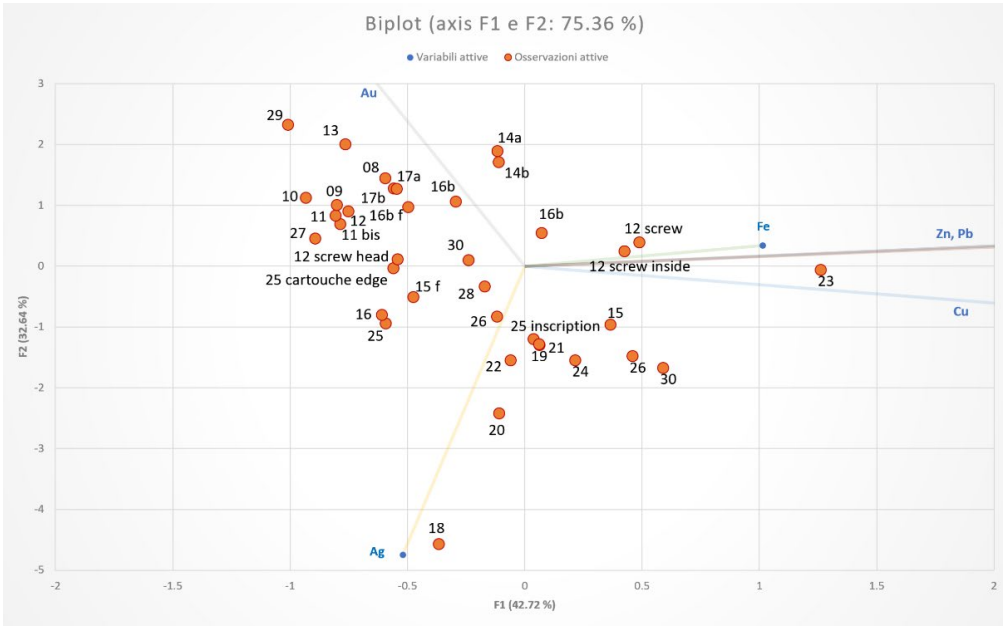

Figure 6. Biplot PC1 vs. PC2 obtained from PCA of the data on metal objects.

A biplot Ag/Au vs. Cu/Au was also produced (Figure 7).

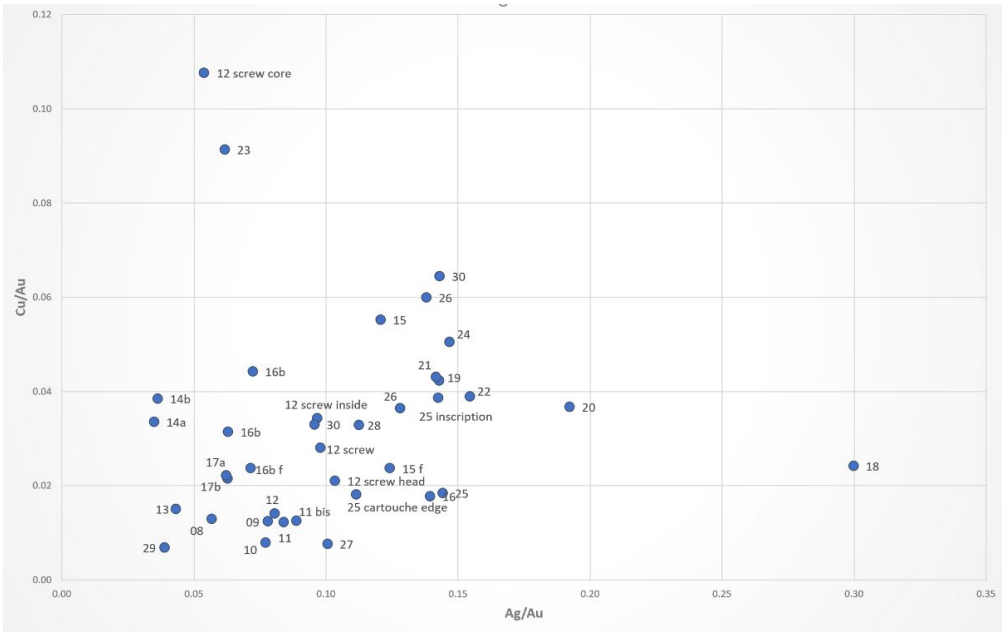

Figure 7. Biplot Ag/Au vs. Cu/Au.

A first group included the objects 19/Ori, 20/Ori, 21/Ori, 22/Ori, 24/Ori, 26/Ori and 30/Ori where the alloys composition was on average as follows: Au/83.8 ± 1.3%, Ag/12.4 ± 1.3%, Cu/3.8 ± 0.8%.

A second group was characterised by higher gold contents, with averages for the three elements equal to: Au/90.6 ± 1.3%, Ag/8.2 ± 1.1%, Cu/1.2 ± 0.4%, this group includeed 9/Ori, 10/Ori, 11/Ori, 12/Ori, 25/Ori (cartouche) and 27/Ori.

The pair of earrings 17a/Ori and 17b/Ori showed the same chemical composition Au/92.2%, Ag/5.8%, Cu/2.0%, practically equal to that of the rod bracelet 8/Ori (Au/92.3%, Ag/5.2%, Cu/1.6%).

The jewel 16/Ori showed a variable composition: the ring (Au/86.4%, Ag/12.0%, Cu/1.5%) was comparable to the first group, whereas the pendant with stones and bezels has Au/90.8 ± 1.0%, Ag/6.3 ± 0.4%, Cu/3.0 ± 0.9%.

The alloy with the highest gold content was that of the pair of polyhedral earrings 14a/Ori and 14b/Ori and 13/Ori unpaired ones that showed compositions with gold almost 95% (Au/93.3 ± 0.4%, Ag/3.3 ± 0.1%, Cu/3.4 ± 0.3%).

The other pair of polyhedral earrings 15a/Ori and 15b/Ori hads an intermediate composition between the first and the second group (Au/86.5 ± 1.3%, Ag/10.3 ± 0.5%, Cu/3.2 ± 1.3%), practically identical to the ring with monogram 28/Ori.

Finally, the composition of the fragmentary wire earring 18/Ori showed a silver content of around 22%, which made us suppose that it was even in front of a golden object. In this case the data should be separated and re-read in the different stratigraphic components.

4. Discussion

As stated in the introduction, the non-invasive diagnostic analyses performed on the Desana treasure have put together a dataset of high relevance, which supports our work hypothesis on the potential of the jewellery deposits for a better characterization of Italian jewellery of the 5th–6th centuries, for the location of its production centre(s) and for the reconstruction of a precise timeline of its artistic and technological evolution, as well as of its economic and cultural implications.

The first observation to be made is that the overall set of raw materials used by Late Antique Italian goldsmiths did not differ essentially from the neighbouring European and Mediterranean regions. Garnets, emeralds, sapphires, amethysts and glass were widely used as part of the decoration of coeval artworks. From that perspective, the jewellery represented at Desana fits comfortably in the main guidelines of Mediterranean goldsmithing. The typology of most of the artefacts as well as the style of the decorations further supports this observation.

This is also true for the pair of bow brooches (objects no. 30/Ori and 31/Ori) with *cloisonné* decoration. Although the essential form of this kind of object is of Central European origin, the specimens from Desana were certainly produced in northern Italy, as the geographical distribution of its closest parallels suggests. The *cloisonné* decoration recreates the typical red-and-green flat panels of the Apahida–Tournai metalwork, using very similar raw materials: Indian almandines and glass of Mediterranean (Roman) origin. Unlike in the Apahida–Tournai group, no Bohemian pyropes have been recorded in the brooches or elsewhere in the Desana treasure.

The set of garnets used in Desana shows indeed some slight differences if compared with coeval jewels recorded north of the Alps. Indian almandines seem to be thus the most frequent gemstones in *cloisonné* artworks of the 5th and 6th centuries on both sides of the Alps. The likely Portuguese garnet recorded in the necklace 20/Ori, however, marks a significant difference between Desana, on the one hand, and the Merovingian territories, on the other; in the latter, as said, such garnets (type IV) were used only from the 7th century onwards. The necklace dates from the late 5th or early 6th century and is likely to have been produced in northern Italy. As the Desana treasure was concealed not later than the mid-6th century and no evidence of modern alteration of the necklace can be conclusively proven; the Portuguese garnet could suggest that Italian workshops were supplied by different distribution networks than their Central European counterparts. In addition to the transcontinental route bringing Indian almandines to the Mediterranean, mid-distance routes may have brought Iberian garnets to Italy. In the current state of research, two main hypotheses can be formulated: either Italy received supplies from the Iberian Peninsula during the 5th–6th century or the Portuguese garnet was an old gemstone at the moment of assembling the necklace 20/Ori. As said, written sources of the 1st century CE attest that the garnet mines at Monte Suímo were being already exploited. This second hypothesis seems to be consistent with the origin of other gemstones used in the necklace, such as the

engraved amethyst. Furthermore, the size and the form of the garnet find better parallels among Roman and Late Antique jewellery than among Portuguese garnets employed in late Merovingian jewellery [47] and in the Guarrazar treasure [27]. A similar explanation can be proposed for the unusual composition of the garnet preserved in the bracelet or diadem 10/Ori, a considerably old object (probably aged not less than 200 years) at the time of the concealment of the treasure. It appears therefore likely that the two outlier garnets arrived in Italy before the period of the great boom of the Asian garnets in the European markets, that is, in the 5th–6th century.

The rest of the analysed gemstones do not significantly modify this general picture. Drop-shaped sapphires were a recurring element in Mediterranean luxury jewellery. Treasures connected to elite groups of metropolises such as Carthage and Rome contained earrings with drop shaped sapphires such as 16/Ori in Desana [48,49]. Dating from the 5th century, the sapphire from Desana, worked with diamond, could have reached Italy through the same trade networks that brought Indian almandines to the Mediterranean. The analysed emeralds fit quite well into this pattern, as they show provenances from Asia, Egypt and Austria. No chronological discrimination of the different provenances can be made on the basis of the Desana objects, although it seems that Egyptian and Indian emeralds were used more often in the late 5th and early 6th century, this is, broadly at the same time as Asian garnets.

Amethysts are less eloquent regarding their provenance, so for now they cannot add further data to this discussion An interesting issue about amethysts is that they experienced a great boom in Mediterranean and European markets between the late 6th and the early 7th century [50]. Before that, their presence was far less frequent. Two of the Desana artefacts having delivered amethysts were probably old objects when they joined the treasure: namely, the already discussed 10/Ori and the capsella 11/Ori. As for the necklace 20/Ori, one of the two amethysts was surely recycled from an old jewel, as its engraved representation suggests. These observations suggest that the presence of amethysts in late 5th—early 6th century Italian jewellery might have been purely occasional, as shown by other coeval assemblages.

As for the glass, it shows the usual features in Roman and Late Antique productions, widely present in Italian markets. The larger number of analysed samples corresponds to green glass with very high percentages of SiO_2. Blue glass has only been detected in silverware items, belonging to the latest period of accumulation of the treasure. It is expected that the increase in data after the analyses on other assemblages of the same period will determine whether this may be a relevant chronological discrimination.

Indian almandines, sapphires, Indian and Egyptian emeralds, and green glass seem to be the basic set of the jewellers of the late 5th and early 6th century. Blue glass seems to appear at a later point, probably after 500 CE. The recorded amethysts and Portuguese garnets, as well as some Pakistani emeralds, seem to belong to Roman times rather than to the 5th–6th century. Therefore, from the viewpoint of supply, the Desana artefacts confirm that northern Italy was well connected to the main trade routes bringing Asian gemstones and beads and Near Eastern glass and gemstones to Europe, as other categories of manufactured goods (e.g., imported pottery) show.

As said, the analysed metal alloys are consistent with the typical compositions of the period. From this viewpoint, thus, they do not modify essentially the picture outlined by glass and gemstones. In addition, they convey relevant data on the composition and on the formation of the treasure. The groups defined by the composition of the Au alloys seem to be consistent with chronological and functional observations. An early group including, among other objects, the crossbow brooch 12/Ori, the openwork bracelet 9/Ori and the "antiques" 10/Ori and 11/Ori shows a chronology stretching from the 3rd/4th century to the mid-5th century. As it is formed by old objects containing about 90% of gold, it can be probably inferred that they were collected and kept mainly because of their intrinsic value. The groups defined by 17/Ori and 8/Ori, on the one hand, and by Ori/20, Ori/21, Ori/30, Ori/31, Ori/19 and Ori/24, on the other, may instead be interpreted as

two broadly coeval jewellery sets dating from the second half of the 5th century or from the very beginning of the 6th century. If this hypothesis is to be followed, the former group would find numerous parallels in treasures and women's graves recorded throughout the Mediterranean basin [51]. The second one, showing brooches of Ponto–Danubian tradition combined with Mediterranean necklaces and finger rings should be included in a rather exclusive group of "barbarian" princely graves scattered between the Danube lands and Northern Africa [51,52]. These data thus add valuable evidence supporting the long and complex formation of the treasure and open new perspectives on the determination of the place and time of production of several types of jewels.

5. Conclusions

In our view, these preliminary results are a good example of the perspectives that our current line of investigation will open in the near future.

It is expected that such dataset will be enlarged as the campaign of analyses scheduled within the project "Upgrading the archaeology of the Odoacrian and Ostrogothic kingdom: archaeometry, bioarchaeology and context analysis" (2022–23) will proceed.

Author Contributions: Conceptualization, J.P.G. and M.G.; methodology, M.A. and A.A.; software, E.C.; validation, A.A., M.L. and E.C.; formal analysis, F.R.; investigation, M.A., F.R., M.L. and A.A.; resources, J.P.G., M.G. and S.C.; data curation, E.C. and F.R.; writing—original draft preparation, M.A. and J.P.G.; writing—review and editing, M.G., S.C. and A.A.; visualization, M.L.; supervision, J.P.G.; project administration, M.G.; funding acquisition, J.P.G. All authors have read and agreed to the published version of the manuscript.

Funding: This research was funded by Specifické vyzkumy of Faculty of Philosophy at Univerzita Hradec Králové (Czech Republic), 2022, entitled "Upgrading the archaeology of the Odoacrian and Ostrogothic kingdom: archaeometry, bioarchaeology and context analysis".

Institutional Review Board Statement: Not applicable.

Informed Consent Statement: Not applicable.

Data Availability Statement: Not applicable.

Acknowledgments: The authors would like to thank Giovanni Carlo Federico Villa, director of Museo Civico di Arte Antica in Torino, for allowing inspection of the Tesoro. Marco Aimone is also gratefully acknowledged for fruitful discussion.

Conflicts of Interest: The authors declare no conflict of interest. The funders had no role in the design of the study; in the collection, analyses, or interpretation of data; in the writing of the manuscript, or in the decision to publish the results.

References

1. Degani, M. *Il Tesoro Romano Barbarico di Reggio Emilia*; Sansoni: Firenze, Italy, 1959.
2. Bierbrauer, V. Die Ostgotischen Funde von Domangnano, Republik San Marino (Italien). *Germania* **1973**, *51*, 499–523.
3. Bierbrauer, V. *Die Ostgotischen Grab- und Schatzfunde in Italien*; Biblioteca; Centro italiano di studi sull'alto Medioevo: Spoleto, Italy, 1975.
4. Bierbrauer, V. Reperti Ostrogoti Provenienti Da Tombe o Tesori Della Lombardia. In *I Longobardi e la Lombardia*; Azzimonti: Milano, Italy, 1978; pp. 213–240.
5. Manière-Lévêque, A.M. L'évolution Des Bijoux "Aristocratiques" Féminins à Travers Les Trésors Proto-Byzantins d'orfèvrerie. *Rev. Archéologique* **1997**, *1*, 79–106.
6. Baldini Lippolis, I. *L'oreficeria Nell'impero di Costantinopoli Tra IV e VII Secolo*; Bibliothec; Edipuglia: Bari, Italy, 1999.
7. Aimone, M. *Il Tesoro Di Desana. Una Fonte per Lo Studio Della Società Romano-Ostrogota in Italia*; BAR Intern; Archaeopress: Oxford, UK, 2010.
8. Baldini Lippolis, I.; Pinar Gil, J. Osservazioni Sul Tesoro Di Reggio Emilia. In Proceedings of the Ipsam Nolam Barbari Vastaverunt: L'Italia e il Mediterraneo Occidentale tra il V Secolo e la Metà del VI, Cimitile-Nola-Santa Maria Capua Vetere, Cimitile, Italy, 18–19 June 2009; Ebanista, C., Rotili, M., Eds.; atti del Convegno Internazionale di Studi. Tavolario: Cimitile, Italy, 2010; pp. 113–128.
9. AA.VV. *Royal Insignia of the Late Antiquity from Mšec and Řevničov, Bohemia*; Jiřík, J., Ed.; V.M.Press: Písek, Czech Republic, 2023.

10. Yatsuk, O.; Ferretti, M.; Gorghinian, A.; Fiocco, G.; Malagodi, M.; Agostino, A.; Gulmini, M. Data from Multiple Portable XRF Units and Their Significance for Ancient Glass Studies. *Molecules* **2022**, *27*, 6068. [CrossRef] [PubMed]
11. Aceto, M.; Calà, E.; Gulino, F.; Gullo, F.; Labate, M.; Agostino, A.; Picollo, M. The Use of UV-Visible Diffuse Reflectance Spectrophotometry for a Fast, Preliminary Authentication of Gemstones. *Molecules* **2022**, *27*, 4716. [CrossRef] [PubMed]
12. De Michele, V.; Aceto, M.; Agostino, A.; Fenoglio, G. La Gemmatura Nella Pace Di Chiavenna. *Arte Lomb.* **2019**, *185*, 72–80. [CrossRef]
13. Gorelick, L.; Gwinnett, A.J. Diamonds from India to Rome and Beyond. *Am. J. Archaeol.* **1988**, *92*, 547–552. [CrossRef]
14. Gwinnett, A.J.; Gorelick, L. A Brief History of Drills and Drilling. *BEADS J. Soc. Bead Res.* **1998**, *10–11*, 49–56.
15. Palanza, V.; Di Martino, D.; Paleari, A.; Spinolo, G.; Prosperi, L. Micro-Raman Spectroscopy Applied to the Study of Inclusions within Sapphire. *J. Raman Spectrosc.* **2008**, *39*, 1007–1011. [CrossRef]
16. Palke, A.C.; Saeseaw, S.; Renfro, N.D.; Sun, Z.; McClure, S.F. Geographic Origin Determination of Blue Sapphire. *Gems Gemol.* **2019**, *55*, 536–579. [CrossRef]
17. Farges, F.; Panczer, G.; Benbalagh, N.; Riondet, G. The Grand Sapphire of Louis XIV and the Ruspoli Sapphire: Historical and Gemological Discoveries. *Gems Gemol.* **2016**, *51*, 392–409. [CrossRef]
18. Schneider, H. *Kosmas Indikopleustes, Christliche Topographie. Textkritische Analysen. Übersetzung. Kommentar*; Brepols Publishers: Turnhout, Italy, 2011.
19. Al-Beruni, M. *The Book Most Comprehensive in Knowledge on Precious Stones*; Said, H.M., Ed.; Adam Publisher: New Delhi, India, 2007.
20. Barone, G.; Mazzoleni, P.; Bersani, D.; Raneri, S. Portable XRF: A Tool for the Study of Corundum Gems. *Open Archaeol.* **2017**, *3*, 194–201. [CrossRef]
21. Kochelek, K.A.; McMillan, N.J.; McManus, C.E.; Daniel, D.L. Provenance Determination of Sapphires and Rubies Using Laser-Induced Breakdown Spectroscopy and Multivariate Analysis. *Am. Mineral.* **2015**, *100*, 1921–1931. [CrossRef]
22. Scarani, A.; Åström, M. Gemological Applications of UV-Vis-NIR Spectroscopy. *Riv. Ital. Gemmol.* **2017**, *7*, 1–9.
23. Saeseaw, S.; Renfro, N.D.; Palke, A.C.; Sun, Z.; McClure, S.F. Geographic Origin Determination of Emerald. *Gems Gemol.* **2019**, *55*, 614–646. [CrossRef]
24. Karampelas, S.; Al-Shaybani, B.; Mohamed, F.; Sangsawong, S.; Al-Alawi, A. Emeralds from the Most Important Occurrences: Chemical and Spectroscopic Data. *Minerals* **2019**, *9*, 561. [CrossRef]
25. Giuliani, G.; Groat, L.A.; Marshall, D.; Fallick, A.E.; Branquet, Y. Emerald Deposits: A Review and Enhanced Classification. *Minerals* **2019**, *9*, 105. [CrossRef]
26. Aurisicchio, C.; Conte, A.M.; Medeghini, L.; Ottolini, L.; De Vito, C. Major and Trace Element Geochemistry of Emerald from Several Deposits: Implications for Genetic Models and Classification Schemes. *Ore Geol. Rev.* **2018**, *94*, 351–366. [CrossRef]
27. Guerra, M.F.; Calligaro, T.; Perea, A. The Treasures of Guarrazar: Tracing the Gold Suppies in the Visigothic Iberian Peninsula. *Archaeometry* **2007**, *49*, 53–74. [CrossRef]
28. Aurisicchio, C.; Corami, A.; Ehrman, S.; Graziani, G.; Cesaro, S.N. The Emerald and Gold Necklace from Oplontis, Vesuvian Area, Naples, Italy. *J. Archaeol. Sci.* **2006**, *33*, 725–734. [CrossRef]
29. Pliny the Elder The Natural History. Available online: http://data.perseus.org/citations/urn:cts:latinLit:phi0978.phi001.perseus-eng1:35.26 (accessed on 30 December 2022).
30. Schmetzer, K.; Gilg, H.A.; Schüssler, U.; Panjikar, J.; Calligaro, T.; Périn, P. The Linkage Between Garnets Found in India at the Arikamedu Archaeological Site and Their Source at the Garibpet Deposit. *J. Gemmol.* **2017**, *35*, 598–627. [CrossRef]
31. Pion, C.; Gratuze, B.; Périn, P.; Calligaro, T. Bead and Garnet Trade between the Merovingian, Mediterranean, and Indian Worlds. In *The Oxford Handbook of The Merovingian World*; Effros, B., Moreira, I., Eds.; Oxford University Press: Oxford, UK, 2020; pp. 819–859.
32. Van Grieken, R.E.; Markowicz, A.A. *Handbook of X-ray Spectrometry*, 2nd ed.; Marcel Dekker: New York, NY, USA, 2002.
33. Rousseau, R. Detection Limit and Estimate of Uncertainty of Analytical XRF Results. *Rigaku J.* **2001**, *18*, 33–46.
34. Gilg, H.A.; Schmetzer, K.; Schussler, U. An Early Byzantine Engraved Almandine from the Garibpet Deposit, Telengana State, India: Evidence for Garnet Trade Along the Ancient Maritime Silk Road. *Gems Gemol.* **2018**, *54*, 149–165. [CrossRef]
35. Raman, K.V. Further Evidence of Roman Trade from Costal Sites in Tamil Nadu. In *Rome and India: The Ancient Sea Trade*; Begley, V., De Puma, R.D., Eds.; University of Wisconsin Press: Madison, WI, USA, 1991; pp. 125–133.
36. Krzemnicki, M.S.; Butini, F.; Butini, E.; De Carolis, E. Gemmological Analysis of a Roman Sapphire Intaglio and Its Possible Origin. *J. Gemmol.* **2019**, *36*, 710–724. [CrossRef]
37. Krzemnicki, M.S.; Hänni, H.A.; Guggenheim, R.; Mathys, D. Investigations on Sapphires from an Alkali Basalt, South West Rwanda. *J. Gemmol.* **1996**, *25*, 90–106. [CrossRef]
38. Gübelin, E.J.; Koivula, J.I. *Photoatlas of Inclusions in Gemstones, Volume 3*; Opinio Publishers: Basel, Switzerland, 2008.
39. Hänni, H.; Schubiger, B.; Kiefert, L.; Häberli, S. Raman Investigations on Two Historical Objects from Basel Cathedral: The Reliquary Cross and Dorothy Monstrance. *Gems Gemol.* **1998**, *34*, 102–125. [CrossRef]
40. Reiche, I.; Pages-Camagna, S.; Lambacher, L. In Situ Raman Spectroscopic Investigations of the Adorning Gemstones on the ReliquaryHeinrich's Cross from the Treasury of Basel Cathedral. *J. Raman Spectrosc.* **2004**, *35*, 719–725. [CrossRef]

41. Agostino, A.; Aceto, M.; Fenoglio, G.; Operti, L. Caratterizzazione Chimica Della Coperta Del Codice C. In *Tabula ornata lapidibus diversorum colorum. La legatura preziosa del Codice C nel Museo del Tesoro del Duomo di Vercelli*; Lomartire, S., Ed.; Viella: Roma, Italy, 2015; pp. 125–162. ISBN 9788867285907.
42. Superchi, M. Le Gemme Dell'Evangeliario Di Ariberto. In *Evangeliario di Ariberto*; Tomei, A., Ed.; Silvana Editore: Milano, Italy, 1999; pp. 149–157.
43. Robotti, S.; Rizzi, P.; Soffritti, C.; Garagnani, G.L.; Greco, C.; Facchetti, F.; Borla, M.; Operti, L.; Agostino, A. Reliability of Portable X-ray Fluorescence for the Chemical Characterisation of Ancient Corroded Copper-tin Alloys. *Spectrochim. Acta Part B At. Spectrosc.* **2018**, *146*, 41–49. [CrossRef]
44. Beck, L.; Bosonnet, S.; Réveillon, S.; Eliot, D.; Pilon, F. Silver Surface Enrichment of Silver–Copper Alloys: A Limitation for the Analysis of Ancient Silver Coins by Surface Techniques. *Nucl. Instrum. Methods Phys. Res. Sect. B Beam Interact. Mater. At.* **2004**, *226*, 153–162. [CrossRef]
45. Corsi, J.; Lo Giudice, A.; Re, A.; Agostino, A.; Barello, F. Potentialities of X-ray Fluorescence Analysis in Numismatics: The Case Study of Pre-Roman Coins from Cisalpine Gaul. *Archaeol. Anthropol. Sci.* **2018**, *10*, 431–438. [CrossRef]
46. Aceto, M.; Agostino, A.; Labate, M. Analisi Chimica Non Invasiva Del "Tesoro Di Como". *Not. Portale Numis. Dello Stato* **2022**, *16*, 223–231.
47. Calligaro, T.; Périn, P. Une Nouvelle Étape Dans La Connaissance Des Grenats de l'orfèvrerie Mérovingienne. Analyse Géochimique et Provenance Des Grenats Ornant Les Chefs-d'oeuvre de l'orfèvrerie Mérovingienne Conservés Au Département Des Monnaies, Médailles et an-Tiques de La Bi. *Antiq. Natl.* **2022**, *52*, 42–71.
48. Ross, M.C. *Catalogue of the Byzantine and Early Mediaeval Antiquities in the Dumbarton Oaks Collection, Vol. 2, Jewelry, Enamels and Art of the Migration Period*; Dumbarton Oaks: Washington, DC, USA, 1965.
49. Baratte, F.; Lang, J.; La Nièce, S.; Metzger, C. *Le Trésor de Carthage. Contribution à l'étude de L'orfèvrerie de l'Antiquité Tardive*; CNRS Editions: Paris, France, 2002.
50. Drauschke, J. Byzantine Jewellery? Amethyst Beads in East and West during the Early Byzantine Period. In *Intelligible Beauty: Recent Research on Byzantine Jewellery*; Entwistle, C., Adams, N., Eds.; British Museum Press: London, UK, 2010; pp. 50–60.
51. Pinar Gil, J. Local Realities and Continental-Wide Fashions. Some Paradoxes on 5th-6th Century Clothing Ornamenta in the Western Mediterranean Provinces (and Beyond). In *Political Fragmentation and Cultural Coherence in Late Antiquity*; Boschung, D., Danner, M., Radtki, C., Eds.; Wilhelm Fink: Munich, Germany; Paderborn, Germany, 2015; pp. 249–290.
52. Pinar Gil, J. Barbarian Jewellery, Social Space, Urban Culture. A Contribution to Fashion Theory in the Early Migration Period (Western Europe, ca. 400-480 AD). *Slov. Archaeol.* **2021**, *69*, 55–97. [CrossRef]